Environmental Science & Technology

Article

Local and regional components of aerosol in a heavily trafficked street canyon in central London derived from PMF and cluster analysis of single particle ATOFMS spectra

Chiara Giorio, Andrea Tapparo, Manuel Dall'Osto, David C.S. Beddows, Johanna Esser-Gietl, Robert M Healy, and Roy Michael Harrison

Environ. Sci. Technol., **Just Accepted Manuscript** • Publication Date (Web): 19 Feb 2015

Just Accepted

Local and regional components of aerosol in a heavily trafficked street canyon in central London derived from PMF and cluster analysis of single particle ATOFMS spectra

Chiara Giorio[1,2*a], Andrea Tapparo[1], Manuel Dall'Osto[3], David C.S. Beddows[2], Johanna K. Esser-Gietl[2,b], Robert M. Healy[4] and Roy M. Harrison[2,5]

[1] Dipartimento di Scienze Chimiche, Università degli Studi di Padova, Via Marzolo 1, 35131 Padova, Italy

[2] National Centre for Atmospheric Science, School of Geography, Earth and Environmental Sciences, Division of Environmental Health and Risk Management, University of Birmingham, Edgbaston, Birmingham B15 2TT, United Kingdom

[3] Marine Science ICM-CSIC, Consejo Superior de Investigaciones Científicas (CSIC), C/ LLuis Solé i Sabarís S/N, 08028 Barcelona, Spain

[4] Southern Ontario Centre for Atmospheric Aerosol Research, University of Toronto, Toronto, Canada

[5] Also at: Department of Environmental Sciences/Center of Excellence in Environmental Studies, King Abdulaziz University, Jeddah, 21589, Saudi Arabia

*corresponding author: Phone: +44 1223 763615; Fax: +44 1223 336362; e-mail: chiara.giorio@atm.ch.cam.ac.uk

[a] present address: Centre for Atmospheric Science, Department of Chemistry, University of Cambridge, Lensfield Road, Cambridge CB2 1EW, United Kingdom

[b] present address: Deutscher Wetterdienst (DWD), Meteorological Observatory, Albin-Schwaiger-Weg 10, Hohenpeissenberg, Germany

ABSTRACT

Positive Matrix Factorization (PMF) has been applied to single particle ATOFMS spectra collected on a six lane heavily trafficked road in central London (Marylebone Road), which well represents an urban street canyon. PMF analysis successfully extracted 11 factors from mass spectra of about 700,000 particles as a complement to information on particle types (from K-means cluster analysis). The factors were associated with specific sources and represent the contribution of different traffic related components (i.e. lubricating oils, fresh elemental carbon, organonitrogen and aromatic compounds), secondary aerosol locally produced (i.e. nitrate, oxidized organic aerosol and oxidized organonitrogen compounds), urban background together with regional transport (aged elemental carbon and ammonium) and fresh sea spray. An important result from this study is the evidence that rapid chemical processes occur in the street canyon with production of secondary particles from road traffic emissions. These locally generated particles, together with aging processes, dramatically affected aerosol composition producing internally mixed particles. These processes may become important with stagnant air conditions and in countries where gasoline vehicles are predominant and need to be considered when quantifying the impact of traffic emissions.

KEYWORDS

Traffic emissions, secondary aerosol, regional contribution, street canyon, positive matrix factorization, ATOFMS, single particle analysis

INTRODUCTION

Airborne particulate matter is one of the major polluting agents in the urban atmosphere, posing a substantial burden for public health.[1-5] Despite air quality guidelines and policies established worldwide, the progress in reducing PM concentrations in urban areas has been slow in recent years. Cost-effective reduction of PM concentrations may be achieved only after investigating and apportioning source contributions using chemistry-transport modeling or receptor modeling methods.[6]

A large fraction of atmospheric aerosol is constituted by organic compounds.[7-12] Nonetheless, the precise mechanisms of formation and evolution of secondary organic aerosol (SOA) are still a subject of research.[13,14] SOA comprises a complex mixture of organic compounds which originates from both local emissions and long range transport, and ages through many reactions and processes, making it difficult to link SOA to a precise emission source.

It is believed that vehicular traffic makes a major contribution to total particulate matter emissions within urban areas, being the main contributor to the observed increase of PM concentrations above the regional background.[15] It is commonly observed that heavily trafficked routes, and especially those within urban canyons, are major hotspots with respect to particle pollution, in which the contributions from regionally transported pollutants, pollutants from the city and emissions from road traffic are superimposed.[15,16] Many studies have demonstrated that both exhaust and non-exhaust (i.e. abrasion, brake, tire and road surface wear, resuspension from the road pavement) contribute to the measured PM concentration, reaching a ratio of 1:1 in the roadside environment.[17-21] Nonetheless, the estimation of non-exhaust emissions is still recognized as a priority area of uncertainty.[22] Quantification of the resuspension of road dust is a key and very difficult task because road dust presents a varied and heterogeneous chemical profile as a result of multiple sources contributing to the accumulation of particles on the road pavement.[23-25]

Estimating the relative source contributions of aerosol can be difficult, especially in the urban environment, requiring advanced measurement techniques able to provide both size and chemical characterization of aerosol with high time resolution.[26-28] Aerosol Time-of-Flight Mass Spectrometry (ATOFMS) is one of the most versatile techniques able to acquire size and chemical characterization of single particles in real time. ATOFMS provides important information on the mixing state of aerosol, but does not readily give quantitative information as it is biased by many sampling artefacts.[29,30] Cluster and factor analytical techniques can be useful approaches to extract qualitative information on particle types and the major chemical components from the large datasets provided by the ATOFMS.[26,31,32] Traditional K-means cluster analysis and ART-2a artificial neural network analysis are able to extract many different particle types which are normally difficult to link to specific aerosol sources.[30] Giorio *et al.*[31] applied Positive Matrix Factorization (PMF) analysis for the first time directly to single particle ATOFMS spectra. PMF analysis proved to be useful at deconvolving single particle mass spectra and extracting the contribution of each component. For example, fresh EC was successfully separated from aged EC, and OC was separated into different organic families such as aromatic compounds, N-containing organic compounds and oxidized organic aerosol in the analysis of rural background aerosol.[31] Factor analysis applied to aerosol mass spectrometry (AMS) data has proved to be effective at extracting and separating simplified organic factors associated with some specific source or chemical process, i.e. primary, secondary, hydrocarbon-like, oxidized and cooking aerosol.[6,33,34] Single particle analysis with a soot particle aerosol mass spectrometer (SP-AMS) separated the contribution of two black carbon particle types internally mixed hydrocarbon-like substances.[35]

In the present study, PMF analysis has been applied, for the first time, to single particle ATOFMS data collected in a heavily trafficked street canyon in central London and the results compared to those derived from K-means cluster analysis. Information on main particle components (from PMF), mixing-state of particles (from K-means cluster analysis), meteorological data, vehicular

traffic flow, gaseous species and PM concentrations and time-series of metals (from ATOFMS data) have been used to assign and apportion the main sources of local, regional or mixed local/regional particle components. The results obtained have been used to elucidate emission sources and processes occurring in the street canyon, among which particular importance appears to be assumed by the locally produced secondary aerosol.

EXPERIMENTAL SECTION

Measurement Site and Instrumentation

The sampling campaign was conducted in London, at Marylebone Road (51.52°N, 0.15°W), a six-lane heavily trafficked road within an urban canyon, between 22nd May and 11th June 2009 (Figure S1, Supporting Information). Sampling instruments were placed in a cabin at the southern curbside, ca. 150 m east of the main junction with Baker Street on the westbound carriageway. Further details of the sampling site can be found elsewhere.[16]

Hourly data for local weather, gaseous pollutants and PM concentrations, were obtained from the London air quality archive (www.londonair.org.uk). Meteorological data from Heathrow Airport, on the outskirts of London, were used in this study because they are representative of winds above the street canyon.[16] Five day air mass back-trajectories arriving at Marylebone Road at three different altitudes (100, 500 and 1000 meters) were acquired using HYSPLIT (Hybrid Single Particle Lagrangian Integrated Trajectory Model).[36] Vehicular traffic flow data were obtained from King's College, London.

During the campaign, an Aerosol Time-of-Flight Mass Spectrometer fitted with an Aerodynamic Focusing Lens system (TSI 3800-100 AFL),[31,37-40] registered 693,462 bipolar mass spectra of single aerosol particles. The data obtained were exported using the TSI MS-Analyze software (section "PMF analysis", Supporting Information) and analyzed using Positive Matrix Factorization (PMF)

and K-means cluster analysis. Corrections for size-dependent transmission losses[29] were not applied as independent size distribution data were not available. Size distributions presented in this paper should therefore be taken as indicative only and used in a comparative rather than absolute sense.

Positive Matrix Factorization (PMF) Analysis

The PMF analysis was conducted using the software PMF2.[41,42] The positive matrix factorization model solves the equation $X=GF+E$ where X is the original $n\times m$ data matrix, G is the $n\times p$ scores matrix (factors weight) and F is the $p\times m$ loadings matrix (factors profile), E represents the $n\times m$ residuals matrix. Absolute areas under the peaks were used for PMF analysis, which was directly applied to single particle mass spectra ($n\times m$ data matrix of n single particles, m variables - m/z values - in which each datum is the absolute area under the peak in the mass spectra corresponding to the n_i particle and m_j m/z signal) following the method optimized by Giorio et al.[31] Further details on PMF analysis are described in the Supporting Information (section "PMF analysis").

Cluster Analysis

ATOFMS particle mass spectra were directly imported into ENCHILADA[43] and all single particle mass spectra were normalized and then clustered using the K-means algorithm with squared Euclidean distance.[44] The 15 cluster solution was selected initially; subsequently a cluster comprised of miscalibrated mass spectra was eliminated and 14 clusters were then considered for the results. Further details are reported in the Supporting Information (section "Cluster analysis and correlation analysis") together with details about correlation analysis and hierarchical cluster analysis.

Diversity

The diversity of the particle population[45,46] has been calculated based on the relative counts of each particle class extracted through k-means cluster analysis. Diversity values vary as a function of time and were calculated at hourly resolution. This approach differs from that described by Healy et al.[45], where single particle mass fractions of chemical species were used to assess diversity instead. Further details can be found in the Supporting Information (section "Diversity").

RESULTS

The results of the PMF analysis are reported in Figure S4, which shows the mass spectra, size distributions, diurnal trends and wind roses associated with the extracted factors. Some of the factors, indicative of the potential sources, are also reported in Figure 1. Similarly, the results of the K-means cluster analysis (Figure S5) and information on other important data (Figure S6) are reported in the Supporting Information.

PMF analysis, directly applied to single particle mass spectra collected in Marylebone Road, London (UK), extracted the contribution of 11 factors (Figure S4) which explain 55% of the variance of the dataset. This value of explained variance is in line with other statistical analyses, such as ART-2a analysis, applied to ATOFMS datasets[31] and the main contribution to residuals is from miscalibrated signals (Figure S2). The factors are:

- F1-K, explaining 6.4% of variance and containing signals of potassium (m/z 39/41);
- F2-NIT, explaining 1.6% of variance and containing signals of nitrate (m/z -46/-62);
- F3-NaCl, explaining 2.8% of variance, characterized by peaks of Na^+ (m/z 23), Na_2^+ (m/z 46), Na_2O^+ (m/z 62), Na_2OH^+ (m/z 63), Na_2Cl^+ (m/z 81/83) and Cl^- (m/z -35/-37);
- F4-OOA, explaining 4.6% of variance, characterized by peaks of $C_2H_3^+$ (m/z 27) and $C_2H_3O^+$ (m/z 43);

- F5-NH4, explaining 1.9% of variance, containing signals of NH_4^+ (m/z 18), NO^+ (m/z 30) and $C_2H_3O^+$/$CHNO^+$ (m/z 43);
- F6-CN, explaining 1.4% of variance, characterized by peaks of CN^- (m/z -26) and CNO^- (m/z -42);
- F7-EC+, explaining 18.7% of variance, characterized by positive fragments of elemental carbon (m/z 12, 24, 36, 48, 60);
- F8-EC- explaining 2.3% of variance, characterized by negative fragments of elemental carbon (m/z -24, -36, -48, -60);
- F9-OC-Arom explaining 9.8% of variance, containing mainly signals related to aromatic compounds (m/z 27, 41, 43, 51, 53, 55, 57, 63, 69, 77, 87, 91, 115);[47]
- F10-OC-CHNO explaining 3.5% of variance, characterized by signals related to N-containing organic compounds (m/z 43, 49-52, 60-63, 84-87);
- F11-Ca explaining 2.0% of variance, characterized by a main peak of Ca^+ at m/z 40 and small peaks of $CaOH^+$ at m/z 57 and Ca_2O^+ at m/z 96.

The clusters extracted from K-means cluster analysis (Figure S5), accounting for 98.7% of the total number of particles, are:

- 1-K-EC-OC-NIT (23.5%), characterized by very intense signals of potassium (m/z 39/41) and minor signals associated with elemental carbon, aromatic and oxidized organic compounds, all isotopes of Pb, nitrate and cyanide;
- 2-OOA-AROM (7.6%), characterized by secondary organic ions ($C_2H_3^+$ and $C_2H_3O^+$) and fragments due to aromatic compounds (m/z 51/55/63);
- 3-Ca-EC (5.1%), characterized mainly by Ca^+ (m/z 40, with ca. 15% interference from K^+) and $CaOH^+$ (m/z 57), Ca_2O^+ (m/z 96) and organic and elemental carbon signals;
- 4-AROM-CN-SUL (1.6%), characterized by aromatic compounds and PAH in the positive mass spectrum and CN^-, CNO^-, nitrate and sulfate in the negative mass spectrum;

- 5-NaCl (7.8%), representing freshly emitted sea spray;
- 6-EC-background (34.0%), characterized by elemental carbon fragments in the positive mass spectrum;
- 7-Amine58 (0.6%) with a strong signal at m/z 58 associated with $C_2H_5NCH_2^+$ and signals associated mainly with primary amines;[48]
- 8-OOA-NIT-SUL (3.4%), characterized by $C_2H_3^+$, $C_2H_3O^+$, nitrate and sulfate;
- 9-OC-K-SOA (6.8%), whose main signals are K^+, $C_2H_3^+$ and $C_2H_3O^+$ in the positive mass spectrum and nitrate and sulfate in the negative mass spectrum;
- 10-K-NIT (3.3%) composed mainly of potassium and nitrate;
- 11-Na-EC (2.4%) composed of Na^+ (m/z 23) and elemental carbon fragments which are more intense in the negative mass spectrum;
- 12-Fe-V (1.7%) formed by V^+, Fe^+ and VO^+ (m/z 51/56/67);
- 13-Amine59 (0.6%) with strong signals associated with trimethylamine (m/z 59), signals related to secondary and tertiary amines,[48] and secondary aerosol components, i.e. ammonium, nitrate, sulfate and OOA (m/z 27/43);
- 14-N-EC (0.3%) composed of an elemental carbon signal in the negative mass spectrum and a strong peak at m/z 42 which could be linked to $C_2H_4N^+$, and small peaks at m/z 84/112/127 linked to amines.[48]

Details of the correlations between PMF factors and K-means clusters and their time-series are described in the Supporting Information (Section “Results”).

Hourly time-series (Figure S3) of the extracted PMF factors (in scores) and clusters (in number of particles) were analyzed through hierarchical cluster analysis (average linkage, *r*-Pearson distance measure). Concerning PMF factors (Table S2, Figure 2a), the results show the division of the factors into four groups: (i) F3-NaCl, which is an independent factor, related to sea spray (ii) F7-EC+ and F5-NH4 factors, from the urban background (iii) F8-EC-, F11-Ca and F6-CN,

representative of primary emissions from road traffic and (iv) organic factors, F1-K and F2-NIT, characterized by mixed local secondary and primary emissions. Also for the clusters (Table S3, Figure 2b), four main groups can be separated: (i) 5-NaCl, which is an independent cluster originated from sea spray, (ii) 6-EC-background, 12-Fe-V and 2 amine clusters related to transport of air from the urban background (iii) 3-Ca-EC, 11-Na-EC and 14-N-EC from primary emissions and (iv) 1-K-EC-OC-NIT, 10-K-NIT and organic clusters, representing a complex mixture originating from primary emissions and local aging processes.

DISCUSSION

The main groups of PMF factors and K-means clusters separated through the hierarchical cluster analysis (Figure 2) are discussed in detail in the following sections.

Traffic Related Primary Emissions

Five PMF factors are significantly correlated to the count of vehicle flow in Marylebone Road (Table 1): F1-K ($r=0.37$, p-value < 0.001), F6-CN ($r=0.28$, p-value < 0.001), F8-EC- ($r=0.24$, p-value < 0.001), F9-OC-Arom ($r=0.24$, p-value < 0.001) and F11-Ca ($r=0.26$, p-value < 0.001). F7-EC+ and F5-NH4 factors are anti-correlated with traffic counts while the other factors are not significantly correlated to traffic counts (p-value > 0.1). In the present campaign, a diurnal trend characterized by two main peaks in the correspondence of rush hours (normally used to depict traffic contribution) was not observed. In fact, the diurnal trend of vehicular traffic flow was stable and intense during the day and decreased only for a few hours in the early morning (2am-4am) (see Figure 1), including during the weekends.

The polar plots confirm the association with vehicular traffic emissions, showing that the contribution of these factors increased when winds blew from the south-westerly direction (Figure

1). Wind speed and direction above the canyon strongly influence the dynamics within the canyon. In particular, when wind speed is > 1-2 m/s a vortex is formed within the canyon while with lower wind speeds, stagnant conditions prevail.[49,50] At the specific sampling site it can be observed that when above-canopy winds blow from the south-easterly direction the traffic contribution is mixed with pollution from the urban background, while with winds from the opposite direction (NW) the urban background contribution is predominant at the sampling point. When above-canopy winds blow from the south-westerly direction a strong traffic contribution is transported from the main junction with Baker Street, often congested, to the sampling point. It has been suggested that traffic congestion significantly increases emissions, to a greater degree than the number of vehicles itself.[51-54]

A similar wind directionality was observed for traffic related gaseous primary pollutants, i.e. NO_x, SO_2 and CO (Figure S6; NO_x appears also in Figure 1). The factors F1-K, F6-CN, F8-EC-, F9-OC-Arom and F11-Ca show moderate[55] correlations with gaseous primary pollutants (Table 1), and with the time-series of some metals measured by the ATOFMS (Sb, Ba, Cu, Zn and Ca; Table S5), identified as known markers of vehicular traffic emissions (Gietl et al. 2010).
During the sampling campaign average traffic distribution was 3% motorcycles, 70% taxis, cars and LGVs (light goods vehicles), 24% minibuses, buses and rigid HGVs (heavy goods vehicles) and 3% articulated HGVs. Diurnal trends of traffic flow were consistent among the different classes. Conversely, diurnal trends of vehicle speed decreased during the daytime hours indicating more congestion at the junction with Baker Street.

F11-Ca and 3-Ca-EC represents a clear vehicular traffic signature from lubricating oils used in vehicle engines.[30] The size distribution is shifted towards smaller particles with a tail in the direction of Aitken mode particles (Figure 1) characteristic of a primary origin from exhaust emissions.

Similarly to F11-Ca, F8-EC- presents a size distribution shifted towards smaller particles. Giorio *et al.*[31] reported for the first time for a regional background site that EC- is related to fresh emissions while EC+ represents aged elemental carbon as an effect of particle composition which affects the ionization and fragmentation pattern of EC.[31,56,57] The same results has been obtained also in this sampling campaign, where F8-EC- is clearly related to fresh emissions from vehicular traffic (Table 1) while F7-EC+ is related to transport of aged particles from the urban background (see section "Urban background and long range transport").

F8-EC- contributes mainly to three different particle types (clusters): 3-Ca-EC (lubricating oils), 11-Na-EC and 14-N-EC. The 11-Na-EC cluster is strongly correlated with the 3-Ca-EC cluster (Figure 2b, Table S3) and could also be associated with exhaust emissions. 14-N-EC is a small cluster (in number of particles) characterized by a mixture of elemental carbon, signals from amines (Figure S5), which have been already measured in exhaust emissions,[58,59] and a large peak at m/z 42. The latter could be an aspecific fragment of higher molecular weight organonitrogen compounds or acetonitrile[60] adsorbed on particle surfaces. Furthermore, amines can be produced by high-temperature surface reactions on soot particle with NH_3 and NO.[59] It has been demonstrated that vehicles running under rich air-fuel conditions with three-way catalytic converters emit NH_3.[61-64]

Factor F9-OC-Arom presents a size distribution centered at ca. 300-400 nm (Figure S4). Its wind rose shows a mixed local-primary traffic signature. F9-OC-Arom is characterized by signals associated with aromatic compounds that are freshly emitted by vehicular traffic. Its diurnal trend depicts a nighttime peak probably because a decrease of temperature favors condensation into the aerosol phase. This can explain the partial local contribution depicted by the wind rose (Figure S4). It represents the freshly emitted components of the 2-OOA-AROM and 8-OOA-NIT-SUL clusters. These two clusters are characterized by primary aromatic compounds (more present in 2-OOA-

AROM) internally mixed with oxidized/aged compounds (more present in 8-OOA-NIT-SUL) and wind roses confirm a mixed primary/local-secondary contribution for the 2-OOA-AROM cluster and a more local secondary contribution for the 8-OOA-NIT-SUL cluster (Figure S5).

A previous study in Marylebone Road found a factor associated with NO_x and winds from the south-westerly direction. Based on its size distribution, in the range 50-200 nm, and wind directionality, it was assigned to "solid carbonaceous particles from diesel exhaust".[16] This factor can be related to F8-EC-, F11-Ca and F9-OC-Arom factors and mainly to the 2-OOA-Arom, 3-Ca-EC, 11-Na-EC and 14-N-EC clusters found in the present study. From fuel sales date for the UK for 2009, the sales of gasoline and diesel were in the approximate ratio 50:50 which is consistent with the observation of high elemental carbon emissions. In other countries, e.g. USA, gasoline vehicles are largely predominant.[65]

The F6-CN factor, like F9-OC-Arom, has a size distribution centered at ca. 300-400 nm (Figure S4). Organonitrogen compounds are known to be emitted by combustion sources,[68] such as exhaust emissions from road traffic. Factor F6-CN contributes to two highly internally mixed particle types: 4-AROM-CN-SUL cluster and 8-OOA-NIT-SUL cluster (Figure S5, Table 2). The 4-AROM-CN-SUL cluster is characterized by fragments related to primary emission from road traffic (i.e. aromatic compounds, PAH, CN^-, CNO^- and elemental carbon) and its wind rose depicts a clear traffic contribution (Figure S5). The presence of sulfate in 4-AROM-CN-SUL and 8-OOA-NIT-SUL (Figure S5) is not related to long range transport of air masses[66,67] but may derive from minor impurities in the motor fuels (estimated average sulfur content of 6.24 ppm in gasoline and 8.43 ppm in diesel sold in the EU in 2009).[65]

The wind roses of F6-CN and 4-AROM-CN-SUL indicate an additional contribution associated with winds from the northerly direction (Figure S4). A previous study suggested an influence from

suburban traffic related to winds from the northerly direction in Marylebone Road.[16] The same contribution can be seen also in the wind rose plots for CO, NO_x, SO_2 (Figure S6, Figure 1) and cluster 11-Na-EC (Figure S5). Thus, an influence from suburban traffic may explain this observation.

Unexpectedly, the wind rose and diurnal trend of F1-K and cluster 1-K-EC-OC-NIT (in which potassium is the main component in all particles) clearly indicate a traffic signature although potassium is normally considered a marker of biomass/biofuel emissions.[69,70] It might be associated in part with road dust resuspension even if its size distribution, centered at 300-400 nm (Figure S4), is not entirely consistent with this hypothesis. Potassium has also been reported as a minor component of diesel and biodiesel exhaust[71,72] and this may be a contributor. Nonetheless, both the diurnal variation and size association seen in Figure S4 are strongly indicative of biomass burning as the main, but not sole contributor. The ATOFMS is extremely sensitive to potassium[73] and thus its detection may be possible even when it is present at trace levels, as those associated with diesel and biodiesel exhaust.[74] It is considered that further studies are required to better quantify the contribution of these various potassium sources to the source apportionment of urban aerosol.

Local Secondary Aerosol

Factors F2-NIT, F4-OOA and F10-OC-CHNO show size distributions centered at ca. 400-500 nm and wind roses that depict a local origin (Figure 1). Their abundance increases at night, with stable boundary layer[50] and stagnant air conditions inside the canyon. Under these conditions, the contribution from the urban background is minimized and transport of pollutants is due mainly to diffusion and local turbulence. The dendrogram in Figure 2a also suggests that F2-NIT, F4-OOA and F10-OC-CHNO are produced inside or close to the street canyon, as they cluster together with factors associated with primary emissions from road traffic. A factor with similar characteristics,

defined as "local night source", was identified from size distribution data in a previous campaign at Marylebone Road.[16]

F2-NIT represents local nitrate, from nitric acid formed locally by oxidation of NO_x emitted by vehicular traffic, which is then neutralized and condenses onto particles. It contributes mainly to the 10-K-NIT cluster, similar to a cluster already observed at an urban background site in London and associated with locally produced secondary aerosol.[75] It contributes also to highly internally mixed organic particles, i.e. 8-OOA-NIT-SUL and 9-OC-K-SOA. Nitrate is usually present in aerosol as ammonium nitrate but can also arise from reactions of alkaline particles such as calcium carbonate with nitric acid.

F4-OOA is chemically very similar to F9-OC-Arom (characterized by fragments of aromatic compounds),[47] and their time-series are strongly correlated (Figure 2a, Table S2). Additionally, the presence of oxidized fragments ($C_2H_3^+$ and $C_2H_3O^+$) in the mass spectrum and strong correlations with particles in which primary and secondary organic compounds are internally mixed (clusters 2-OOA-AROM, 8-OOA-NIT-SUL and 9-OC-K-SOA, Table 2) suggest that F4-OOA represents aged aromatic compounds formed from primary emissions from vehicular traffic. F4-OOA could be formed by ozonolysis of olefinic compounds or photochemical aging with OH radical and NOx. The contribution of F4-OOA increased during night hours (Figure 1). This can be explained as an effect of decreasing temperature which favors condensation onto particles or a contribution from dark ozonolysis reactions.[12]

The F10-OC-CHNO factor contains both N-containing organic compounds and oxygenated N-containing organic compounds. It may be formed by reaction of primary emitted organic compounds (from road traffic) which underwent photochemical aging promoted by NOx and night chemistry promoted by NO_3 radical.[12,76] Another possible mechanism of formation could be linked

to reactions between carboxylic acids and primary emitted amines or ammonia[64,77,78] or oxidation of these species by OH radical, NO_x and O_3.[59]

F10-OC-CHNO is associated mainly with the cluster 9-OC-K-SOA, whose wind rose depicts a mixed local/urban background contribution (Figure S5). The dendrogram in Figure 2b and correlations with factors associated with primary emissions suggest that 9-OC-K-SOA can be associated with secondary organic aerosol produced predominantly in or close to the street canyon with a small contribution from transport from the background of the city.

An important result from the present study is that rapid aging processes, with production of secondary aerosol, occur in or close to street canyons, as indicated by the lack of directionality and association with low wind speeds in the wind rose (polar) plots for clusters 8, 9 and 10 (Figure S5). This observation is supported by smog chamber experiments on oxidation of anthropogenic VOCs[79-81] and laboratory data in which primary emissions from gasoline vehicles produced SOA in a time scale of a few hours after exposure to ·OH at relevant concentration level expected in the urban environment.[82] In addition, the lack of correlation of F2-NIT and F4-OOA with RH ($r=0.02$ and 0.07 for F2-NIT and F4-OOA respectively, $p>0.12$) suggests that these factors are formed predominantly by secondary processes in the gas phase rather than aging of primary particles which is kinetically dependent upon uptake of ·OH in the particle phase.[83,84] Conversely, F10 OC-CHNO is weakly correlated with RH ($r=0.21$, $p<0.001$) and may be formed from both gas-phase and particle-phase oxidation processes. These processes contribute to the complexity of the clusters observed, by producing highly internally mixed particles (e.g. 8-OOA-NIT-SUL and 9-OC-K-SOA).

Another important aspect is that during stagnant conditions (wind speed < 1-2 m/s), the estimated contribution of secondary aerosol produced locally increased from 12% to 17% (indicative percentage in number of particles, from data non-corrected for size-dependent inlet efficiency,

Table 3). This means that locally produced secondary aerosol needs to be taken into account as a contributor from traffic emissions in addition to primary components. This is particularly important in countries were gasoline vehicles are predominant,[82] e.g. in the USA.[65]

Diversity values for the particle population support this observation. As shown in Figure 1, local emissions increase the diversity of the population by adding their contribution to the urban background. Diversity increases as the day progresses and during nighttime suggesting that aging processes and secondary aerosol formation lead to a more diverse particle population overall. On the contrary, at a rural background site in Harwell (UK) diversity values did not show any particular diurnal trend and were impacted instead by long range transport episodes (Figure S7).

Bulk analysis on low time resolution samples could misinterpret these secondary components and associate them with transport from the urban background instead of traffic emissions. Thus, PMF analysis on single particle data has proved to be useful in elucidating the aging processes occurring in street canyons.

The rapid formation of organic aerosol on a spatial scale from 34 m to 285 m from a major highway north of Toronto, Canada was recently reported by Stroud *et al.*[85]. The formation mechanism was not elucidated, but our observations give an indication of the likely chemical composition of the particles.

Urban background and Long Range Transport

Factors F7-EC+ and F5-NH4 increase when winds blow from the SE and NW directions, which means that a vortex is formed within the canyon, background air is transported inside the canyon, driving a pure background contribution (NW) or mixed traffic-background contribution (SE) to the sampling site. Their size distributions are centered at ca. 500-600 nm (Figure 1, Figure S4), but F7-

EC+ has a small tail towards the Aitken mode particles identifiable with a contribution to the 11-Na-EC cluster (Figure S5).

Air mass back-trajectories show episodes of long range transport from continental Europe in the periods 25-26/05/2009, 31/05-03/06/2009 and 10-11/06/2009 (Figure S8). In those periods the PM was enriched in F7-EC+ and F5-NH4 factors and 6-EC-background and 12-Fe-V clusters, consistent with a contribution from long-range transport of aged particles.[31,86,87] This could not be the sole source of F7-EC+ which was one of the major contributing factors in this campaign. Transport to the UK of air masses from central Europe is typically associated with an increase of sulfate[66,67] but in this ATOFMS dataset the sulfate signal is scarcely represented (<1%) and it is probably associated with minor impurities in motor fuels.

Other clusters related to urban background air are 7-Amine58 and 13-Amine59 (Figures S5). A comparison between the mass spectra of these two clusters can be found in the supporting information (Figure S9). The cluster 7-Amine58 is associated with winds from the northerly sector. Its diurnal trend depicts a nighttime signature (Figure S5) and it is not strongly correlated to any other cluster (Figure 2b, Table S3). It may be related to biogenic emissions or emissions from the London Zoo, transported from Regent's Park (north of the site). Cluster 13-Amine59 is characterized by a main peak of trimethylamine at m/z 59 [48] and it is internally mixed with secondary components. Previous studies found an association of trimethylamine with many different anthropogenic activities, e.g. industry, livestock, automobiles and tobacco smoke.[59] In ambient aerosol, an association with secondary components, i.e. ammonium, nitrate and sulfate, has already been observed by Zhang *et al.* [88]. In this campaign, trimethylamine was associated with urban background factors (Figure 2b, Table 2), peaking during daytime (Figure S5) and increasing with long range transport from central Europe. Thus, it was linked with regional aged aerosol, from anthropogenic emissions, but a contribution from vehicle emissions was not observed.

A previous study[16] in Marylebone Road extracted three background factors from size distribution data. A "background accumulation mode" factor may be related to F5-NH4 and partially to 9-OC-K-SOA cluster (mixed local/urban background origin). An "aged regional aerosol" giving a major contribution to background air in London may be related to F7-EC+, 6-EC-background and 12-Fe-V cluster. Finally, a "regionally transported particles" category with a daytime signature may be related to cluster 13-Amine59.

Sea spray

The NaCl (factor and cluster) represents the sea spray source, with a size distribution characterized by a coarse mode (Figure S4). Primary particles from sea spray undergo chemical processing in the atmosphere, causing chloride depletion in which nitrate and sulfate substitute chloride in the particles.[89] The 5-NaCl cluster does not contain nitrate signals and the nitrate factor does not show a coarse mode, and hence NaCl is concluded to be freshly produced by marine sources.

PM concentrations in Marylebone Road and relative contribution of local and regional components

Marylebone Road is a hotspot for PM pollution in which vehicular traffic is the main factor contributing to the observed increase of PM concentrations above the regional background.[15] Above-canopy winds strongly influence the transport of pollutant in the street canyon and can change the composition of aerosol measured at the sampling site (Table 3). PM_{10} and $PM_{2.5}$ concentrations in Marylebone Road were higher with above-canopy winds blowing from the south-westerly and south-easterly directions (Table 3) which mean that vehicular traffic emissions (SW) or mixed regional/vehicular traffic contributions (SE) were transported to the sampling site. Stagnant air conditions (wind speed < 1-2 m/s) promote formation of secondary aerosol from oxidation of primary emissions from road traffic. The ratio of $PM_{2.5}/PM_{10}$ in Marylebone Road was

0.72 on average while it was 0.62 at the North Kensington urban background site. This is consistent with a major contribution from exhaust emissions and secondary aerosol which increases the proportion of fine particles.

In Marylebone Road, non-volatile PM_{10} is well correlated to PMF factors representative of primary traffic emissions (Table 1) and presents medium-to-weak correlations with F3-NaCl. The wind rose suggests a link with both traffic emissions and marine sources (Figure S6). Non-volatile $PM_{2.5}$ shows moderate correlations with factors representative of primary emissions from road traffic and factors representative of urban background components (Table 1). Its wind rose confirms that it is generated by mixed traffic/background sources (Figure S6). Volatile PM_{10} and volatile $PM_{2.5}$ are correlated mainly with transport of background air into the street canyon (Figure S6). This is could be due to an association with more volatile regional secondary components (i.e. F5-NH4) rather than aged elemental carbon itself (F7-EC+).

The present study shows the benefits of source attribution using high time resolution and wide range chemical characterization data. PMF applied to single particle data has proven useful to disaggregate the contribution of different sources, fresh and aged aerosol components, and different families of organic compounds, as a complement to information on particle types alone which are a complex superimposition of different contributions.[30] Information on wind roses, traffic flow, gaseous species, PM concentrations and particle diversity were used to assign the sources and elucidate processes occurring in the street canyon. The factors extracted represent the contribution of different traffic related primary components (F11-Ca, F8-EC-, F6-CN, F9-OC-Arom and F1-K), secondary aerosol produced locally (F2-NIT, F4-OOA and F10-OC-CHNO), urban background and long range transport (F7-EC+ and F5-NH4) and fresh sea spray (F3-NaCl).

An important result from this study is that aging processes occur in and close to street canyons, with production of secondary aerosol from traffic related primary emissions. This contribution may

become important under stagnant air conditions (above-canopy winds < 1-2 m/s) and in countries where gasoline vehicles are predominant, for example in the USA.

ASSOCIATED CONTENT

Supporting Information: Additional experimental details and results, including 9 Figures and 6 tables. This material is available free of charge via the Internet at http://pubs.acs.org/.

ACKNOWLEDGEMENTS

Authors thank David Green from King's College London for providing vehicular traffic flow data, Rina Guadagnini for helpful editing of TOC image, Ricardo Suarez-Bertoa for helpful discussion and three anonymous referees for helpful revision of the manuscript.

REFERENCES

(1) CAFE, 2011. Loss in life expectancy attributable to exposure to fine particulate matter. The Clean Air For Europe (CAFE) reference documents. http://ec.europa.eu/environment/archives/cafe/general/pdf/map_pm.pdf. (Accessed October 27, 2014)

(2) Chong, U.; Yim, S. H. L.; Barrett, S. R. H.; Boies, A. M. Air quality and climate impacts of alternative bus technologies in greater London. *Environ. Sci. Technol.* **2014**, 48, 4613-4622.

(3) Harrison, R. M.; Giorio, C.; Beddows, D. C. S.; Dall'Osto, M. Size distribution of airborne particles controls outcome of epidemiological studies. *Sci. Tot. Environ.* **2010**, 409, 289-293.

(4) Raaschou-Nielsen, O.; Andersen, Z. J.; Beelen, R.; Samoli, E.; Stafoggia, M.; Weinmayr, G.; Hoffmann, B.; Fischer, P.; Nieuwenhuijsen, M. J.; Brunekreef, B.; Xun, W. W.; Katsouyanni, K.; Dimakopoulou, K.; Sommar, J.; Forsberg, B.; Modig, L.; Oudin, A.; Oftedal, B.; Schwarze, P. E.; Nafstad, P.; DeFaire, U.; Pedersen, N. L.; Östenson, C.-G.; Fratiglioni, L.; Penell, J.; Korek, M.; Pershagen, G.; Eriksen, K. T.; Sørensen, M.; Tjønneland, A.; Ellermann, T.; Eeftens, M.; Peeters, P. H.; Meliefste, K.; Wang, M.; Bueno-de-Mesquita, B.; Key, T. J.; deHoogh, K.; Concin, H.; Nagel, G.; Vilier, A.; Grioni, S.; Krogh, V.; Tsai, M.-Y.; Ricceri, F.; Sacerdote, C.; Galassi, C.; Migliore, E.; Ranzi, A.; Cesaroni, G.; Badaloni, C.; Forastiere, F.; Tamayo, I.; Amiano, P.; Dorronsoro, M.; Trichopoulou, A.; Bamia, C.; Vineis, P.; Hoek, G. Air pollution and lung cancer incidence in 17 European cohorts: prospective analyses from the European study of cohorts for air pollution effects (ESCAPE). *Lancet Oncol.* **2013**, 14, 813–822.

(5) Yim, S. H. L.; Barrett, S. R. H. Public health impacts of combustion emissions in the United Kingdom. *Environ. Sci. Technol.* **2012**, 46, 4291-4296.

(6) Zhang, Q.; Jimenez, J. L.; Canagaratna, M. R.; Ulbrich, I. M.; Ng, N. L.; Worsnop, D. R.; Sun, Y. Understanding atmospheric organic aerosols via factor analysis of aerosol mass spectrometry: a review. *Anal. Bioanal. Chem.* **2011**, 401, 3045-3067.

(7) Denjean, C.; Formenti, P.; Picquet-Varrault, B.; Katrib, Y.; Camredon, M.; Pangui, E.; Zapf, P.; Giorio, C.; Tapparo, A.; Monod, A.; Siekmann, F.; Decorse, P.; Mangeney, C.; Aumont, B.; Doussin, J. F. Relating hygroscopicity, optical properties and chemical composition of secondary organic aerosol from α-pinene ozonolysis. *Atmos. Chem. Phys. Discuss.* **2014**, 14, 10543-10596.

(8) Giorio, C.; Tapparo, A.; Scapellato, M. L.; Carrieri, M.; Apostoli, P.; Bartolucci, G. B. Field comparison of a personal cascade impactor sampler, an optical particle counter and CEN-EU standard methods for PM10, PM2.5 and PM1 measurement in urban environment. *J. Aerosol Sci.* **2013**, 65, 111-120.

(9) Jimenez, J. L.; Canagaratna, M. R.; Donahue, N. M.; Prevot, A. S.; Zhang, Q.; Kroll, J. H.; DeCarlo, P. F.; Allan, J. D.; Coe, H.; Ng, N. L.; Aiken, A. C.; Docherty, K. S.; Ulbrich, I. M.; Grieshop, A. P.; Robinson, A. L.; Duplissy, J.; Smith, J. D.; Wilson, K. R.; Lanz, V. A.; Hueglin, C.; Sun, Y. L.; Tian, J.; Laaksonen, A.; Raatikainen, T.; Rautiainen, J.; Vaattovaara, P.; Ehn, M.; Kulmala, M.; Tomlinson, J. M.; Collins, D. R.; Cubison, M. J.; Dunlea, E. J.; Huffman, J. A.; Onasch, T. B.; Alfarra, M. R.; Williams, P. I.; Bower, K.; Kondo, Y.; Schneider, J.; Drewnick, F.; Borrmann, S.; Weimer, S.; Demerjian, K.; Salcedo, D.; Cottrell, L.; Griffin, R.; Takami, A.; Miyoshi, T.; Hatakeyama, S.; Shimono, A.; Sun, J. Y.; Zhang, Y. M.; Dzepina, K.; Kimmel, J. R.; Sueper, D.; Jayne, J. T.; Herndon, S. C.; Trimborn, A. M.; Williams, L. R.; Wood, E. C.; Middlebrook, A. M.; Kolb, C. E.; Baltensperger, U.; Worsnop, D. R. Evolution of organic aerosols in the atmosphere. *Science* **2009**, 326, 1525-1529.

(10) Kourtchev, I.; Fuller, S. J.; Giorio, C.; Healy, R. M.; Wilson, E.; O'Connor, I.; Wenger, J. C.; McLeod, M.; Aalto, J.; Ruuskanen, T. M.; Maenhaut, W.; Jones, R.; Venables, D. S.; Sodeau, J. R.; Kulmala, M.; Kalberer, M. Molecular composition of biogenic secondary organic aerosols using ultrahigh resolution mass spectrometry: comparing laboratory and field studies. *Atmos. Chem. Phys.* **2014**, 14, 1-13.

(11) Kourtchev, I.; O'Connor, I. P.; Giorio, C.; Fuller, S. J.; Kristensen, K.; Maenhaut, W.; Wenger, J. C.; Sodeau, J. R.; Glasius, M.; Kalberer, M. Effects of anthropogenic emissions on the molecular composition of urban organic aerosols: An ultrahigh resolution mass spectrometry study. *Atmos. Environ.* **2014**, 89, 525-532.

(12) Rincón, A. G.; Calvo, A. I.; Dietzel, M.; Kalberer, M. Seasonal differences of urban organic aerosol composition - an ultra-high resolution mass spectrometry study. *Environ. Chem.* **2012**, 9, 298-319.

(13) Ehn, M.; Thornton, J. A.; Kleist, E.; Sipilä, M.; Junninen, H.; Pullinen, I.; Springer, M.; Rubach, F.; Tillmann, R.; Lee, B.; Lopez-Hilfiker, F.; Andres, S.; Acir, I. H.; Rissanen, M.; Jokinen, T.; Schobesberger, S.; Kangasluoma, J.; Kontkanen, J.; Nieminen, T.; Kurtén, T.; Nielsen, L. B.; Jørgensen, S.; Kjaergaard, H. G.; Canagaratna, M.; Maso, M. D.; Berndt, T.; Petäjä, T.; Wahner, A.; Kerminen, V. M.; Kulmala, M.; Worsnop, D. R.; Wildt, J.; Mentel, T. F. A large source of low-volatility secondary organic aerosol. *Nature* **2014**, 506, 476-479.

(14) Hallquist, M.; Wenger, J. C.; Baltensperger, U.; Rudich, Y.; Simpson, D.; Claeys, M.; Dommen, J.; Donahue, N. M.; George, C.; Goldstein, A. H.; Hamilton, J. F.; Herrmann, H.; Hoffmann, T.; Iinuma, Y.; Jang, M.; Jenkin, M. E.; Jimenez, J. L.; Kiendler-Scharr, A.; Maenhaut, W.; McFiggans, G.; Mentel, T. F.; Monod, A.; Prévôt, A. S. H.; Seinfeld, J. H.; Surratt, J. D.; Szmigielski, R.; Wildt, J. The formation, properties and impact of secondary organic aerosol: current and emerging issues. *Atmos. Chem. Phys.* **2009**, 9, 5155-5236.

(15) Charron, A.; Harrison, R. M.; Quincey, P. What are the sources and conditions responsible for exceedences of the 24h PM10 limit value (50 µg m^{-3}) at a heavily trafficked London site? *Atmos. Environ.* **2007**, 41, 1960-1975.

(16) Harrison, R. M.; Beddows, D. C. S.; Dall'Osto, M. PMF Analysis of wide-range particle size spectra collected on a major highway. *Environ. Sci. Technol.* **2011**, 45, 5522-5528.

(17) Gietl, J. K.; Lawrence, R.; Thorpe, A. J.; Harrison, R. M. Identification of brake wear particles and derivation of a quantitative tracer for brake dust at a major road. *Atmos. Environ.* **2010**, 44, 141-146.

(18) Harrison, R. M.; Yin, J.; Mark, D.; Stedman, J.; Appleby, R. S.; Booker, J.; Moorcroft, S. Studies of the coarse particle (2.5-10µm) component in UK urban atmospheres. *Atmos. Environ.* **2001**, 21, 3667-3679.

(19) Harrison, R. M.; Dall'Osto, M.; Beddows, D. C. S.; Thorpe, A. J.; Bloss, W. J.; Allan, J. D.; Coe, H.; Dorsey, J. R.; Gallagher, M.; Martin, C.; Whitehead, J.; Williams, P. I.; Jones, R. L.; Langridge, J. M.; Benton, A. K.; Ball, S. M.; Langford, B.; Hewitt, C. N.; Davison, B.; Martin, D.; Petersson, K. F.; Henshaw, S. J.; White, I. R.; Shallcross, D. E.; Barlow, J. F.; Dunbar, T.; Davies, F.; Nemitz, E.; Phillips, G. J.; Helfter, C.; Di Marco, C. F.; Smith, S. Atmospheric chemistry and physics in the atmosphere of a developed megacity (London): An overview of the REPARTEE experiment and its conclusions. *Atmos. Chem. Phys.* **2012**, 12, 3065-3114.

(20) Querol, X.; Alastuey, A.; Ruiz, C. R.; Artiñano, B.; Hansson, H. C.; Harrison, R. M.; Buringh, E.; Ten Brink, H. M.; Lutz, M.; Bruckmann, P.; Straehl, P.; Schneider, J. Speciation and origin of PM10 and PM2.5 in selected European cities. *Atmos. Environ.* **2004**, 38, 6547-6555.

(21) Thorpe, A. J.; Harrison, R. M.; Boulter, P. G.; McCrae, I. S. Estimation of particle resuspension source strength on a major London Road. *Atmos. Environ.* **2007**, 41, 8007-8020.

(22) AQEG, 2005. Particulate matter in the United Kingdom. Report of the UK Air Quality Expert Group, AQEG. Prepared for the Department for Environment, Food and Rural Affairs, the Scottish Executive, the Welsh Assembly Government and the Department of the Environment in Northern Ireland. http://archive.defra.gov.uk/environment/quality/air/airquality/publications/particulate-matter/documents/pm-summary.pdf. (Accessed October 27, 2014)

(23) Amato, F.; Pandolfi, M.; Viana, M.; Querol, X.; Alastuey, A.; Moreno, T. Spatial and chemical patterns of PM_{10} in road dust deposited in urban environment. *Atmos. Environ.* **2009**, 43, 1650-1659.

(24) Amato, F.; Pandolfi, M.; Escrig, A.; Querol, X.; Alastuey, A.; Pey, J.; Perez, N.; Hopke, P. K. Quantifying road dust resuspension in urban environment by Multilinear Engine: a comparison with PMF2. *Atmos. Environ.* **2009**, 43, 2770-2780.

(25) Thorpe, A.; Harrison, R. M. Sources and properties of non-exhaust particulate matter from road traffic: A review. *Sci. Tot. Environ.* **2008**, 400, 270-282.

(26) Jeong, C.-H.; McGuire, M. L.; Godri, K. J.; Slowik, J. G.; Rehbein, P. J. G.; Evans, G. J. Quantification of aerosol chemical composition using continuous single particle measurements. *Atmos. Chem. Phys.* **2011**, 11, 7027-7044.

(27) Pekney, N. J.; Davidson, C. I.; Bein, K. J.; Wexler, A. S.; Johnston, M. V. Identification of sources of atmospheric PM at the Pittsburgh supersite, Part I: single particle analysis and filter-based positive matrix factorization. *Atmos. Environ.* **2006**, 40, S411-S423.

(28) Wexler, A. S.; Johnston, M. V. What have we learned from highly time-resolved measurements during EPA's supersites program and related studies? *J. Air Waste Manag. Assoc.* **2008**, 58, 303-319.

(29) Dall'Osto, M.; Harrison, R. M.; Beddows, D. C. S. Single-particle efficiencies of aerosol time-of flight mass spectrometry during the North Atlantic marine boundary layer experiment. *Environ. Sci. Technol.* **2006**, 40, 5029-5035.

(30) Dall'Osto, M.; Harrison, R. M. Urban organic aerosols measured by single particle mass spectrometry in the megacity of London. *Atmos. Chem. Phys.* **2012**, 12, 4127-4142.

(31) Giorio, C.; Tapparo, A.; Dall'Osto, M.; Harrison, R. M.; Beddows, D. C. S.; Nemitz, E.; Di Marco, C. Comparison of three techniques for analysis of data from an aerosol time-of-flight mass spectrometer. *Atmos. Environ.* **2012**, 61, 316-326.

(32) McGuire, M. L.; Jeong, C. H.; Slowik, J. G.; Chang, R. Y. W.; Corbin, J. C.; Lu, G.; Mlhele, C.; Rehbein, P. J. G.; Sills, D. M. L.; Abbatt, J. P. D.; Brook, J. R.; Evans, G. J. Elucidating determinants of aerosol composition through particle-type-based receptor modelling. *Atmos. Chem. Phys.* **2011**, 11, 8133-8155.

(33) Crippa, M.; De Carlo, P. F.; Slowik, J. G.; Mohr, C.; Heringa, M. F.; Chirico, R.; Poulain, L.; Freutel, F.; Sciare, J.; Cozic, J.; Di Marco, C. F.; Elsasser, M.; Nicolas, J. B.; Marchand, N.; Abidi, E.; Wiedensohler, A.; Drewnick, F.; Schneider, J.; Borrmann, S.; Nemitz, E.; Zimmermann, R.; Jaffrezo, J.-L.; Prévôt, A. S. H.; Baltensperger, U. Wintertime aerosol chemical composition and source apportionment of the organic fraction in the metropolitan area of Paris. *Atmos. Chem. Phys.* **2013**, 13, 961-981.

(34) Healy, R. M.; Sciare, J.; Poulain, L.; Crippa, M.; Wiedensohler, A.; Prévôt, A. S. H.; Baltensperger, U.; Sarda-Estève, R.; McGuire, M. L.; Jeong, C.-H.; McGillicuddy, E.; O'Connor, I. P.; Sodeau, J. R.; Evans, G. J.; Wenger, J. C. Quantitative determination of carbonaceous particle mixing state in Paris using single-particle mass spectrometer and aerosol mass spectrometer measurements. *Atmos. Chem. Phys.* **2013**, 13, 9479-9496.

(35) Lee, A. K. Y.; Willis, M. D.; Healy, R. M.; Onasch, T. B.; Abbatt, J. P. D. Single particle characterization using the soot particle aerosol mass spectrometer (SP-AMS). *Atmos. Chem. Phys. Discuss.* **2014**, 14, 15323-15361.

(36) Draxler, R. R.; Rolph, G. D. HYSPLIT (Hybrid Single-Particle Lagrangian Integrated Trajectory) model v 4.9, NOAA Air Resource Laboratory, Silver Spring MD., 2003; http://ready.arl.noaa.gov/HYSPLIT.php (Accessed October 27, 2014).

(37) Dall'Osto, M.; Beddows, D. C. S.; Kinnersley, R. P.; Harrison, R. M. Characterization of individual airborne particles by using aerosol time-of-flight mass spectrometry at Mace Head, Ireland. *J. Geophys. Res. Atmos.* **2004**, 109, D21302, DOI: 10.1029/2004JD004747.

(38) Drewnick, F.; Dall'Osto, M.; Harrison, R. M. Characterization of aerosol particles from grass mowing by joint deployment of ToF-AMS and ATOFMS instruments. *Atmos. Environ.* **2008**, 42, 3006-3017.

(39) Gard, E.; Mayer, J. E.; Morrical, B. D.; Dienes, T.; Fergenson, D. P.; Prather, K. A. Real-time analysis of individual atmospheric aerosol particles: design and performance of a portable ATOFMS. *Anal. Chem.* **1997**, 69, 4083-4091.

(40) Su, Y.; Sipin, M. F.; Furutani, H.; Prather, K. A. Development and characterization of an aerosol time-of-flight mass spectrometer with increased detection efficiency. *Anal. Chem.* **2004**, 76, 712-719.

(41) Paatero, P. User's Guide for Positive Matrix Factorization Programs PMF2 and PMF3, **1998**.

(42) Paatero, P.; Tapper, U. Positive matrix factorization: a non-negative factor model with optimal utilization of error estimates of data values. *Environmetrics* **1994**, 5, 111-126.

(43) Gross, D. S.; Atlas, R.; Rzeszotarski, J.; Turetsky, E.; Christensen, J.; Benzaid, S.; Olson, J.; Smith, T.; Steinberg, L.; Sulman, J.; Ritz, A.; Anderson, B.; Nelson, C.; Musicant, D. R.; Chen, L.; Snyder, D. C.; Schauer, J. J. Environmental chemistry through intelligent atmospheric data analysis. *Environ. Modell. Softw.* **2010**, 25, 760-769.

(44) MacQueen, J., 1967. Some methods for classification and analysis of multivariate observations. In: Proceedings of 5-th Berkeley Symposium on Mathematical Statistics and Probability, vol.1. University of California Press, Berkeley, pp. 281-297.

(45) Healy, R. M.; Riemer, N.; Wenger, J. C.; Murphy, M.; West, M.; Poulain, L.; Wiedensohler, A.; O'Connor, I. P.; McGillicuddy, E.; Sodeau, J. R.; Evans, G. J. Single particle diversity and mixing state measurements. *Atmos. Chem. Phys.* **2014**, 14, 6289-6299.

(46) Riemer, N.; West, M. Quantifying aerosol mixing state with entropy and diversity measures. *Atmos. Chem. Phys.* **2013**, 13, 11423–11439.

(47) McLafferty, F. W.1983. Interpretation of Mass Spectra, third ed.; CA University Co. Books: Valley, 1983.

(48) Angelino, S.; Suess, D. T.; Prather, K. A. Formation of aerosol particles from reactions of secondary and tertiary alkylamines: characterization by aerosol time-of-flight mass spectrometry. *Environ. Sci. Technol.* **2001**, 35, 3130-3138.

(49) Vardoulakis, S.; Fisher, B. E. A.; Pericleous, K.; Gonzalez-Flesca, N. Modelling air quality in street canyons: a review. *Atmos. Environ.* **2003**, 37, 155-182.

(50) Charron, A.; Harrison, R. M. Fine ($PM_{2.5}$) and coarse ($PM_{2.5\text{-}10}$) particulate matter on a heavily trafficked London highway: sources and processes. *Environ. Sci. Technol.* **2005**, 39, 7768-7776.

(51) Atkinson, R. W.; Barratt, B.; Armstrong, B.; Anderson, H. R.; Beevers, S. D.; Mudway, I. S.; Green, D.; Derwent, R. G.; Wilkinson, P.; Tonne, C.; Kelly, F. J. The impact of the congestion charging scheme on ambient air pollution concentrations in London. *Atmos. Environ.* **2009**, 43, 5493–5500.

(52) Beevers, S. D.; Carslaw, D. C. The impact of congestion charging on vehicle emissions in London. *Atmos. Environ.* **2005**, 39, 1–5.

(53) Jones, A. M.; Harrison, R. M. Estimation of the emission factors of particle number and mass fractions from traffic at a site where mean vehicle speeds vary over short distances. *Atmos. Environ.* **2006**, 40, 7125-7137.

(54) Keogh, D. U.; Kelly, J.; Mengersen, K. L.; Jayaratne, R.; Ferreira, L.; Morawska, L. Derivation of motor vehicle tailpipe particle emission factors suitable for modelling urban fleet emissions and air quality assessments. *Environ. Sci. Pollut. Res.* **2010**, 17, 724-739.

(55) Cohen, J., 1988. Statistical Power Analysis for the Behavioral Sciences. Lawrence Erlbaum Associates Inc., New Jersey, USA.

(56) Reilly, P. T. A.; Lazar, A. C.; Gieray, R. A.; Whitten, W. B.; Ramsey, J. M. The elucidation of charge-transfer-induced matrix effects in environmental aerosols via real-time aerosol mass spectral analysis of individual airborne particles. *Aerosol Sci. Tech.* **2000**, 33, 135-152.

(57) Reinard, M. S.; Johnston, M. V. Ion formation mechanism in laser desorption ionization of individual particles. *J. Am. Soc. Mass Spectrom.* **2008**, 19, 389-399.

(58) Cadle, S. H.; Mulawa, P. A. Low molecular weight aliphatic amines in exhaust from catalyst-equipped cars. *Environ. Sci. Technol.* **1980**, 14, 718-723.

(59) Ge, X.; Wexler, A. S.; Clegg, S. L. Atmospheric amines - Part I. A review. *Atmos. Environ.* **2011**, 45, 524-546.

(60) Holzinger, R.; Jordan, A.; Hansel, A.; Lindinger, W. Automobile emissions of acetonitrile: assessment of its contribution to the global source. *J. Atmos. Chem.* **2001**, 38, 187-193.

(61) Fraser, M. P.; Cass, G. R. Detection of Excess Ammonia Emissions from In-Use Vehicles and the Implications for Fine Particle Control. *Environ. Sci. Technol.* **1998**, 32, 1053-1057.

(62) Sutton, M. A.; Dragosits, U.; Tang, Y. S.; Fowler, D.; Ammonia emissions from non-agricultural sources in the UK. *Atmos. Environ.* **2000**, 34, 855-869.

(63) Tanner, P. Vehicle-related ammonia emissions in Hong Kong. *Environ. Chem. Lett.* **2009**, 7, 37–40.

(64) Suarez-Bertoa, R.; Zardini, A. A.; Astorga, C. Ammonia exhaust emissions from spark ignition vehicles over the New European Driving Cycle. *Atmos. Environ.* **2014**, 97, 43-53.

(65) REPORT FROM THE COMMISSION TO THE EUROPEAN PARLIAMENT AND THE COUNCIL Quality of petrol and diesel fuel used for road transport in the European Union: Eighth annual report (Reporting year 2009). http://eur-lex.europa.eu/legal-content/EN/TXT/?uri=CELEX:52011DC0127 (Accessed November 18, 2014)

(66) Martin, C. L.; Allan, J. D.; Crosier, J.; Choularton, T. W.; Coe, H.; Gallagher, M. W. Seasonal variation of fine particulate composition in the centre of a UK city. *Atmos. Environ.* **2011**, 45, 4379-4389.

(67) Abdalmogith, S. S.; Harrison, R. M. The use of trajectory cluster analysis to examine the long-range transport of secondary inorganic aerosol in the UK. *Atmos. Environ.* **2005**, 39, 6686-6695.

(68) Miller, J. A.; Bowman C. T. Mechanism and modeling of nitrogen chemistry in combustion. *Prog. Energy Combust. Sci.* **1989**, 15, 287–338.

(69) Cheng, Y.; Engling, G.; He, K.-B.; Duan, F.-K.; Ma, Y.-L.; Du, Z.-Y.; Liu, J.-M.; Zheng, M.; Weber, R. J. Biomass burning contribution to Beijing aerosol. *Atmos. Chem. Phys.* **2013**, 13, 7765-7781.

(70) Guazzotti, S. A.; Suess, D. T.; Coffee, K. R.; Quinn, P. K.; Bates, T. S.; Wisthaler, A.; Hansel, A.; Ball, W. P.; Dickerson, R. R.; Neusüß, C.; Crutzen, P. J.; Prather, K. A. Characterization of carbonaceous aerosols outflow from India and Arabia: Biomass/biofuel burning and fossil fuel combustion. *J. Geophys. Res.* **2003**, 108 (D15), 4485, doi:10.1029/2002JD003277.

(71) Dallmann, T. R.; Onasch, T. B.; Kirchstetter, T. W.; Worton, D. R.; Fortner, E. C.; Herndon, S. C.; Wood, E. C.; Franklin, J. P.; Worsnop, D. R.; Goldstein, A. H.; Harley, R. A. Characterization of particulate matter emissions from on-road gasoline and diesel vehicles using a soot particle aerosol mass spectrometer. *Atmos. Chem. Phys. Discuss.* **2014**, 14, 4007-4049.

(72) De Caland, L. B.; Silveira, E. L. C.; Tubino, M. Determination of sodium, potassium, calcium and magnesium cations in biodiesel by ion chromatography. *Anal.Chim. Acta* **2012**, 718, 116–120.

(73) Gross, D. S.; Galli, M. E.; Silva, P. J.; Prather, K. A. Relative sensitivity factors for alkali metal and ammonium cations in single-particle aerosol time-of-flight mass spectra. *Anal. Chem.* **2000**, 72, 416-422.

(74) Cross, E. S.; Sappok, A.; Fortner, E. C.; Hunter, J. F.; Jayne, J. T.; Wong, V. W.; Trimborn, A.; Worsnop, D. R.; Kroll, J. H.; Brooks, W. A.; Onasch, T. B. Real-time measurements of engine-out trace elements: application of a novel soot particle aerosol mass spectrometer for emissions characterization. *J. Eng. Gas Turbines Power* **2012**, 134, 072801.

(75) Dall'Osto, M.; Harrison, R. M.; Coe, H.; Williams, P. I.; Allan J. D. Real time chemical characterization of local and regional nitrate aerosols. *Atmos. Chem. Phys.* **2009**, 9, 3709-3720.

(76) Day, D. A.; Liu, S.; Russell, L. M.; Ziemann, P. J. Organonitrate group concentrations in submicron particles with high nitrate an organic fractions in coastal southern California. *Atmos. Environ.* **2010**, 44, 1970-1979.

(77) Pratt, K. A.; Hatch, L. E.; Prather, K. A. Seasonal volatility dependence of ambient particle phase amines. *Environ. Sci. Technol.* **2009**, 43, 5276-5281.

(78) Vehkamäki, H. Classical nucleation theory in multicomponent systems; Springer: New York, 2006.

(79) Paulsen, D., Dommen, J., Kalberer, M., Prévôt, A. S. H., Richter, R., Sax, M., Steinbacher, M., Weingartner, E., Baltensperger, U. Secondary organic aerosol formation by irradiation of 1,3,5-trimethylbenzene-NOx-H2O in a new reaction chamber for atmospheric chemistry and physics. *Environ. Sci. Technol.* **2005**, 39, 2668-2678.

(80) Volkamer, R., Jimenez, J. L., San Martini, F., Dzepina, K., Zhang, Q., Salcedo, D., Molina, L. T., Worsnop, D. R., Molina, M. J. Secondary organic aerosol formation from anthropogenic air pollution: Rapid and higher than expected. *Geophys. Res. Lett.* **2006**, 33, L17811, doi:10.1029/2006GL026899.

(81) Emanuelsson, E. U., Hallquist, M., Kristensen, K., Glasius, M., Bohn, B., Fuchs, H., Kammer, B., Kiendler-Scharr, A., Nehr, S., Rubach, F., Tillmann, R., Wahner, A., Wu, H.-C., Mentel, Th. F. Formation of anthropogenic secondary organic aerosol (SOA) and its influence on biogenic SOA properties. *Atmos. Chem. Phys.* **2013**, 13, 2837-2855.

(82) Platt, S. M.; El Haddad, I.; Zardini, A. A.; Clairotte, M.; Astorga, C.; Wolf, R.; Slowik, J. G.; Temime-Roussel, B.; Marchand, N.; Ježek, I.; Drinovec, L.; Močnik, G.; Möhler, O.; Richter, R.; Barmet, P.; Bianchi, F.; Baltensperger, U.; Prévôt, A. S. H. Secondary organic aerosol formation from gasoline vehicle emissions in a new mobile environmental reaction chamber. *Atmos. Chem. Phys.* **2013**, 13, 9141-9158.

(83) Bedjanian, Y., Nguyen, M. L., Le Bras, G. Kinetics of the reactions of soot surface-bound polycyclic aromatic hydrocarbons with the OH radicals. *Atmos. Environ.* **2010**, 44, 1754-1760.

(84) Slade, J. H., Knopf, D. A. Multiphase OH oxidation kinetics of organic aerosol: the role of particle phase state and relative humidity. *Geophys. Res. Lett.* **2014**, 41, 5297-5306.

(85) Stroud, C.A.; Liggio, J.; Zhang, J.; Gordon, M.; Staebler, R.M.; Makar, P.A.; Zhang, J.; Li, S.-M.; Mihele, C.; Lu, G.; Wang, D.K.; Wentzell, J.; Brook, J.R.; Evans, G.J. Rapid organic aerosol formation downwind of a highway: Measured and model results from the FEVER study. *J. Geophys. Res. Atmos.* **2014**, 119, 1663-1679.

(86) Dall'Osto, M.; Ovadnevaite, J.; Ceburnis, D.; Martin, D.; Healy, R. M.; O'Connor, I. P.; Kourtchev, I.; Sodeau, J. R.; Wenger, J. C.; O'Dowd, C. Characterization of urban aerosol in Cork city (Ireland) using aerosol mass spectrometry. *Atmos. Chem. Phys.* **2013**, 13, 4997-5015.

(87) de Foy, B.; Smyth, A. M.; Thompson, S. L.; Gross, D. S.; Olson, M. R.; Sager, N.; Schauer, J. J. Sources of nickel, vanadium and black carbon in aerosols in Milwaukee. *Atmos. Environ.* **2012**, 59, 294-301.

(88) Zhang, G.; Bi, X.; Chan, L. Y.; Li, L.; Wang, X.; Feng, J.; Sheng, G.; Fu, J.; Li, M.; Zhou, Z. Enhanced trimethylamine-containing particles during fog events detected by single particle aerosol mass spectrometry in urban Guangzhou China. *Atmos. Environ.* **2012**, 55, 121-126.

(89) Zhao, Y.; Gao, Y. Acidic species and chloride depletion in coarse aerosol particles in the US east coast. *Sci. Tot. Environ.* **2008**, 407, 541-547.

Table 1. Coefficient of correlation (r) values between time series of PMF factors and other available data including gaseous species concentrations, PM concentrations[a] and count of vehicle flow[b].

Concentration of gas species, PM and count of vehicle flow	r (PMF factors vs. other data)										
	K	NIT	NaCl	OOA	NH4	CN	EC+	EC-	OC-Arom	OC-CHNO	Ca
CO	**0.37**	-0.08	0.06	0.18	-0.07	**0.41**	0.08	**0.44**	0.25	-0.02	**0.55**
NOx	**0.28**	-0.08	0.08	0.16	-0.04	**0.36**	0.13	**0.49**	0.22	-0.02	**0.53**
SO_2	**0.30**	-0.06	0.05	0.07	-0.09	**0.33**	0.08	**0.30**	0.14	-0.03	**0.42**
O_3	**-0.27**	-0.16	-0.08	**-0.36**	-0.18	**-0.33**	**-0.28**	**-0.47**	**-0.37**	**-0.27**	**-0.43**
PM_{10}	0.18	-0.02	0.06	0.12	0.10	**0.27**	**0.29**	**0.41**	0.15	0.01	**0.45**
$PM_{2.5}$	0.15	-0.02	-0.05	0.11	0.12	0.18	**0.26**	**0.32**	0.11	-0.02	**0.35**
Volatile PM_{10}	-0.24	-0.10	-0.21	-0.20	0.17	-0.11	**0.43**	0.09	-0.21	-0.11	-0.06
Volatile $PM_{2.5}$	**-0.29**	-0.15	-0.12	**-0.25**	0.13	-0.20	**0.40**	0.01	**-0.26**	-0.15	-0.14
Non-volatile PM_{10}	0.24	-0.01	0.10	0.17	0.07	**0.31**	0.22	**0.42**	0.20	0.03	**0.50**
Non-volatile $PM_{2.5}$	0.21	0.01	-0.03	0.16	0.10	0.22	0.20	**0.33**	0.17	0.00	**0.38**
Traffic flow	**0.37**	0.00	0.09	0.08	-0.18	**0.28**	**-0.28**	0.24	0.24	-0.07	**0.26**

[a] Gaseous species and PM concentrations were expressed in $\mu g/m^3$

[b] Traffic flow data were expressed in number of vehicles/hour

Correlations of medium intensity (r>0.25) are highlighted in bold green, anticorrelations of medium intensity are highlighted in bold red (r<-0.25)

Table 2. Coefficient of correlation (r) values of the linear regressions between hourly time series of PMF factors (equivalent number of particles) and K-means clusters.

PMF factors	r (PMF factors vs K-means clusters)													
	1-K-EC-OC-NIT	2-OOA-AROM	3-Ca-EC	4-Arom-PAH-CN	5-NaCl	6-EC-background	7-Amine58	8-OOA-NIT-SUL	9-OC-K-SOA	10-K-NIT	11-Na-EC	12-Fe-V	13-Amine59	14-N-EC
F1-K	**0.99**	**0.81**	0.36	0.28	-0.01	-0.03	0.20	**0.78**	**0.59**	**0.57**	0.23	-0.07	0.05	0.34
F2-NIT	**0.60**	0.43	0.08	0.31	-0.16	0.21	0.28	**0.73**	**0.67**	**0.96**	0.17	0.19	0.14	0.22
F3-NaCl	0.04	0.13	0.21	0.12	**0.96**	-0.36	-0.06	-0.05	-0.08	-0.11	0.15	-0.33	-0.22	0.07
F4-OOA	**0.73**	**0.83**	0.41	0.40	-0.06	0.27	0.40	**0.83**	**0.80**	**0.61**	0.33	0.25	0.27	0.44
F5-NH4	0.26	0.14	-0.12	0.16	-0.28	**0.74**	0.37	0.47	**0.78**	0.48	0.04	**0.67**	**0.56**	0.18
F6-CN	**0.64**	**0.71**	**0.68**	**0.54**	0.08	-0.01	0.27	**0.58**	0.45	**0.52**	**0.59**	-0.04	0.04	0.48
F7-EC+	-0.06	-0.11	-0.19	0.05	-0.37	**1.00**	0.38	0.10	0.38	0.13	0.08	**0.83**	0.50	0.16
F8-EC-	0.08	0.29	0.34	0.34	-0.16	**0.67**	**0.51**	0.27	0.44	0.35	**0.62**	**0.58**	0.43	0.45
F9-OC-Arom	**0.82**	**0.86**	0.47	0.41	0.03	0.05	0.31	**0.91**	**0.76**	**0.66**	0.32	0.05	0.14	0.44
F10-OC-CHNO	0.37	0.34	0.07	0.34	-0.19	**0.64**	0.42	**0.58**	**0.86**	**0.64**	0.26	**0.57**	0.44	0.30
F11-Ca	0.23	0.44	0.47	0.28	0.04	0.18	0.27	0.32	0.28	0.27	**0.64**	0.15	0.10	0.38

Strong correlations (r>0.5) are highlighted in bold/green.

Table 3. Comparison between average PM concentrations in North Kensington (urban background site), in Marylebone Road (roadside site) and indicative percentage contribution of primary emissions, local secondary, regional and clean/marine components with different above-canopy wind conditions derived from PMF analysis of ATOFMS data in Marylebone Road during the sampling campaign in May-June 2009.

Above-canopy winds	**Wind direction**	**Stagnant**	**NE**	**SE**	**SW**	**NW**
	Wind speed (m/s)	**< 1.5**	**> 1.5**	**> 1.5**	**> 1.5**	**> 1.5**
North Kensington (Urban background)	**PM_{10} (µg/m^3)**	18.8	19.9	23.0	18.3	15.3
	$PM_{2.5}$ (µg/m^3)	14.0	11.1	14.6	10.6	9.9
	ratio $PM_{2.5}/PM_{10}$	0.74	0.60	0.64	0.56	0.60
Marylebone Road (Roadside)	**PM_{10} (µg/m^3)**	21.7	18.8	**31.9**	**38.2**	23.6
	$PM_{2.5}$ (µg/m^3)	17.4	14.5	**28.0**	**27.7**	18.2
	ratio $PM_{2.5}/PM_{10}$	**0.78**	0.70	0.75	0.70	0.70
% contribution of the different components[a] in Marylebone Road	**Primary**	42	39	37	**56**	38
	SOA local	**17**	12	12	15	12
	Regional	36	39	**47**	20	**45**
	Clean/Marine	5	**10**	4	9	5
	Total	100	100	100	100	100

[a] indicative percentage contributions derived from PMF factors in equivalent number of particles.
Highest PM concentrations, ratio $PM_{2.5}/PM_{10}$, and percentage contribution of each component in Marylebone Road according to different wind conditions are highlighted in bold.

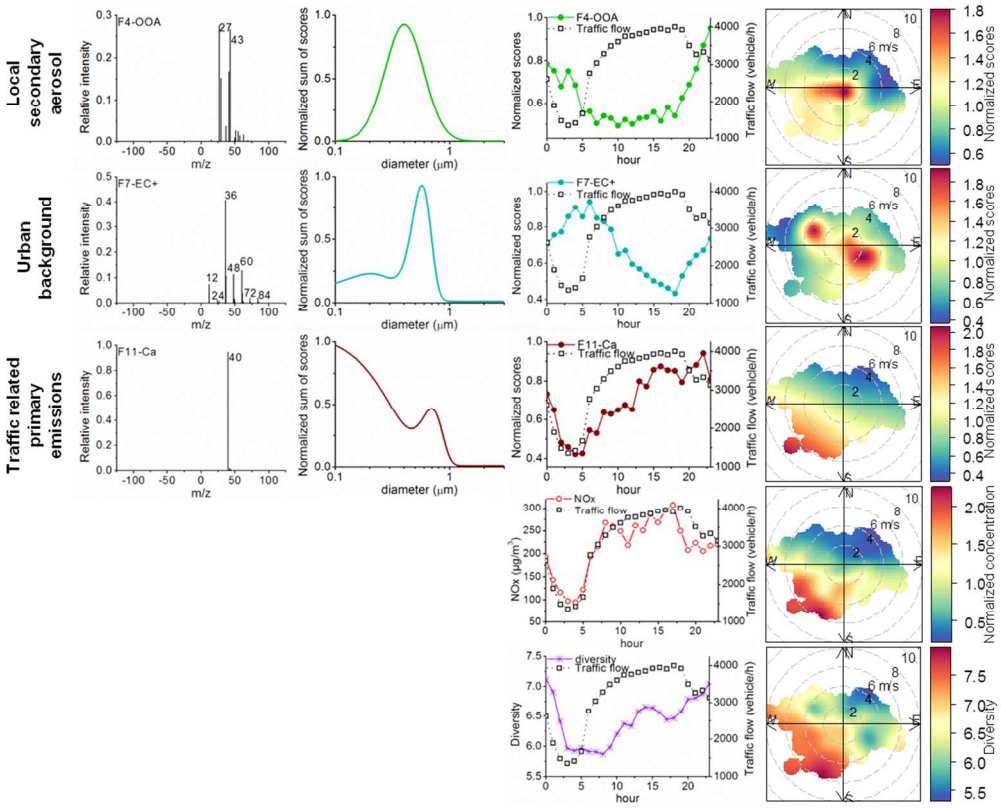

Figure 1. PMF results derived from single particle mass spectra collected at Marylebone Road, London (UK). For each extracted factor the mass spectrum, average size distribution, average diurnal trend, wind rose depicting the trend in scores (normalized) with wind speed and direction are reported. In addition, diurnal trend and wind roses for NOx (as a reference of road traffic related emissions) and particle diversity are reported at the bottom rows. Average uncertainty for diurnal trends is ca. 60%.
201x163mm (150 x 150 DPI)

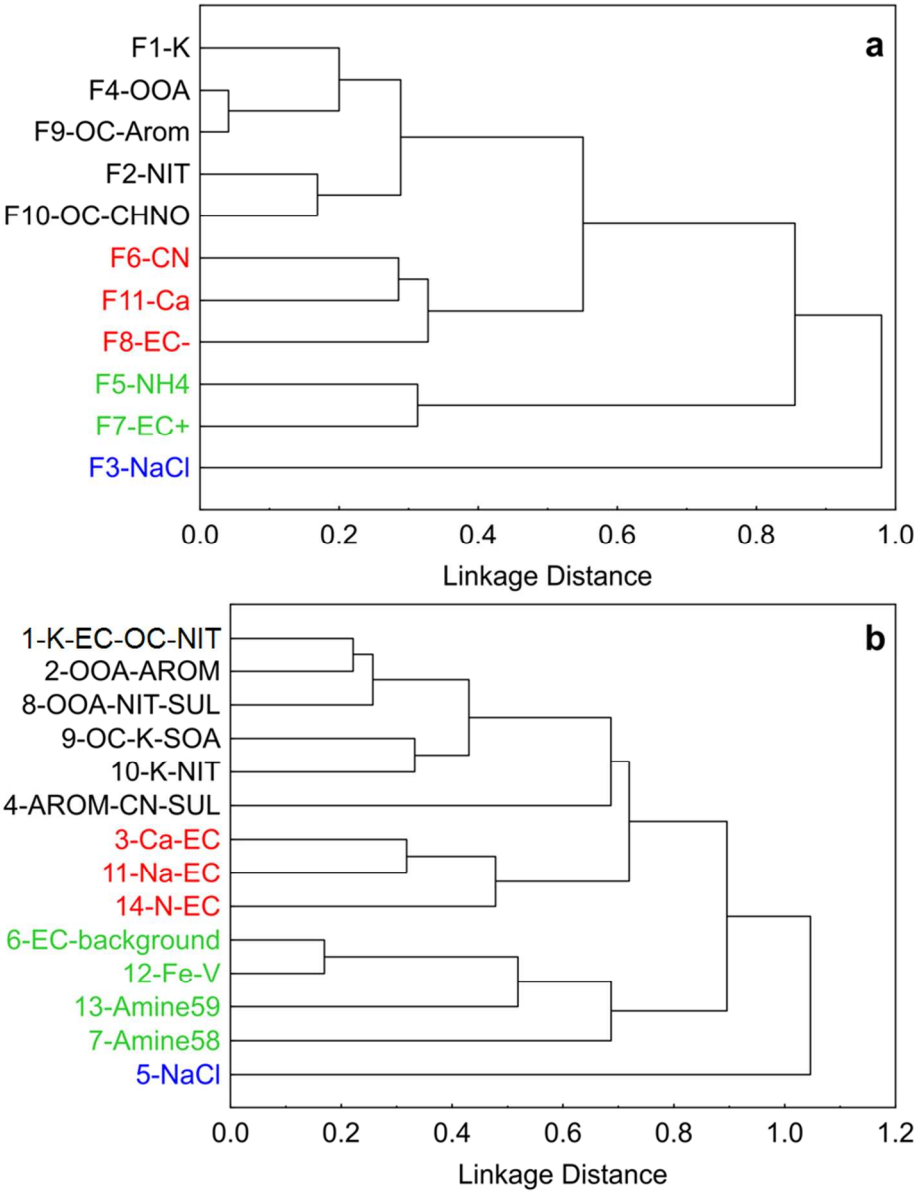

Figure 2. Dendrogram obtained from the hierarchical cluster analysis applied to (a) the time-series of the PMF factors and (b) the time series of k-means clusters (average linkage method, r-Pearson correlation coefficient distance measure). The different colors indicate the separation of variables into different groups. 250x323mm (96 x 96 DPI)

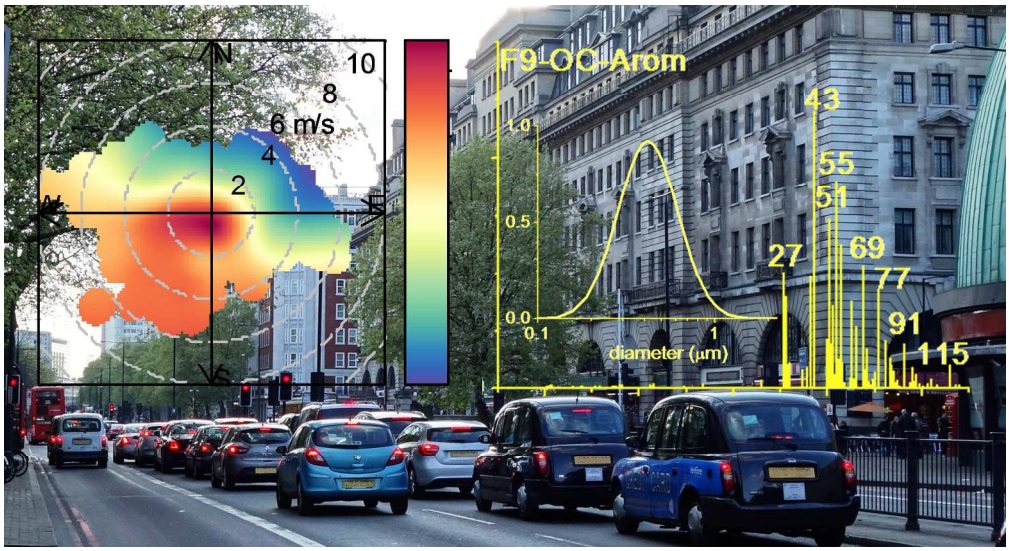

266x143mm (300 x 300 DPI)